

# N-Heterocyclic Carbene Boranes as Electron-Donating and Electron-Accepting Components of $\pi$ -Conjugated Systems\*\*

Kazuhiko Nagura, Shohei Saito, Roland Fröhlich, Frank Glorius,\* and Shigehiro Yamaguchi\*

N-Heterocyclic carbenes (NHCs)<sup>[1]</sup> react with trivalent boranes to form Lewis base/acid complexes.<sup>[2]</sup> In the past several years, this chemistry has attracted increasing attention. Various useful NHC–boranes for organic synthesis have been reported, such as hydrogen-radical donors,<sup>[3]</sup> hydride sources,<sup>[4]</sup> substrates for cross-coupling reactions,<sup>[5]</sup> organo-catalysts,<sup>[6]</sup> and frustrated Lewis pairs.<sup>[7]</sup> In addition, the removal of a substituent from the tetracoordinated boron in NHC–boranes produces intriguing tricoordinated boron species, such as borenium ions,<sup>[8]</sup> boryl radicals,<sup>[9]</sup> and boryl anions.<sup>[10]</sup> However, studies of NHC–boranes from a materials point of view have been limited to only a few examples. Piers and co-workers reported NHC-coordinated boraacenes with small HOMO–LUMO gaps, in which a saturated NHC moiety plays a key role in the stabilization of the boraacene skeletons, but does not fully participate in the  $\pi$  conjugation because of the orthogonal conformation.<sup>[11]</sup> An unsaturated NHC-bearing borabenzene with a coplanar geometry was also reported by Herberich and co-workers, in which, however, the borabenzene and the NHC ring are not noticeably conjugated to each other as a result of their different electronic characters.<sup>[12]</sup>

We were interested in the potential of NHC–boranes as components of  $\pi$ -conjugated skeletons. While many NHC ligands with two aryl groups on the nitrogen atoms have been synthesized, these aryl groups are introduced in order to control the steric bulkiness of the ligands and suppress dimerization, but do not significantly conjugate with the NHC moiety because of their almost orthogonal conformations. In contrast, the introduction of a boryl group to the *ortho* positions of the N-aryl groups should fix the aryl–NHC skeleton in a coplanar fashion, and thereby the aryl ring and the NHC ring can fully conjugate to each other (Figure 1). We

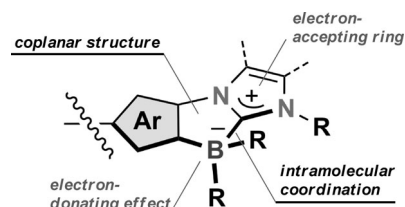
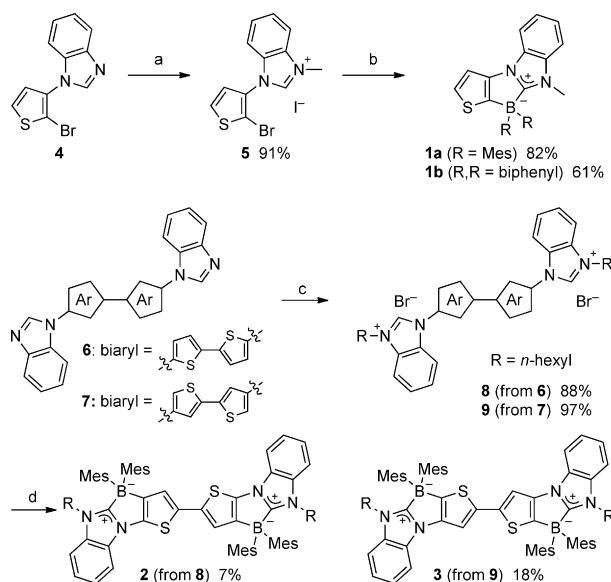


Figure 1. Electronic effects of the NHC–borane moiety.

envisioned in this structure that the zwitterionic character of the NHC–borane moiety endows the aryl  $\pi$  skeleton not only with a highly polar character, but also with a highly electron-donating character, because the borate moiety is a strong electron-donating group. At the same time, the NHC ring acts as an electron-accepting moiety because of its cationic character. In order to investigate the impacts of these multifaceted electronic features, we chose thiophene and bithiophene as representative aryl  $\pi$  skeletons. A series of NHC–borane-substituted derivatives, **1–3**, have been synthesized and their reactivity and properties have been studied.

NHC–borane-substituted thiophenes **1a** and **1b**, which bear a dimesitylboryl and a dibenzoborolyl group as boron moiety, respectively, were successfully obtained by a two-step synthesis from benzimidazolylthiophene **4** (Scheme 1). In the



Scheme 1. Synthesis of **1–3**. Reagents and conditions: a) MeI, CH<sub>2</sub>Cl<sub>2</sub>, 50°C; b) *n*BuLi (2 equiv), diethyl ether, –78°C→0°C, then Mes<sub>2</sub>BF or bromodibenzoborole; c) bromohexane, PhCN, 150°C; d) LDA (4 equiv), THF, –78°C→0°C, then Mes<sub>2</sub>BF.

[\*] K. Nagura, Dr. S. Saito, Prof. Dr. S. Yamaguchi  
Department of Chemistry, Graduate School of Science  
Nagoya University  
Furo, Chikusa, Nagoya 464-8602 (Japan)  
E-mail: yamaguchi@chem.nagoya-u.ac.jp  
Dr. R. Fröhlich, Prof. Dr. F. Glorius  
Organisch-Chemisches Institut  
Westfälische Wilhelms-Universität Münster  
Corrensstrasse 40, 48149 Münster (Germany)  
E-mail: glorius@uni-muenster.de

[\*\*] This work was supported by a Grant-in-Aid (No. 19675001) from the Ministry of Education, Culture, Sports, Science, and Technology (Japan), CREST, JST, and the Deutsche Forschungsgemeinschaft (IRTG Münster-Nagoya). K.N. thanks the JSPS Research Fellowship for Young Scientists.

Supporting information for this article is available on the WWW under <http://dx.doi.org/10.1002/anie.201204050>.

first step, **4** was converted to imidazolium salt **5** by alkylation with an excess of MeI. The deprotonation and halogen/lithium exchange reaction of **5** were simultaneously accomplished by treatment with two equivalents of *n*BuLi to produce the corresponding NHC with a lithiated thienyl group. The following reaction with Mes<sub>2</sub>BF or bromodibenzoborole afforded products **1a** and **1b** as stable colorless compounds. In a similar manner,  $\pi$ -expanded bithiophenes **2** and **3**, which have two NHC moieties at the 5,5' and 4,4' positions of the bithiophene skeleton, respectively, were also synthesized from bis(benzimidazolyl)bithiophene precursors **6** and **7**, in which the hexyl groups were introduced to gain sufficient solubility, and four equivalents of LDA were used to simultaneously deprotonate the imidazolium and thiophene rings. The yields of **2** and **3** were only moderate, partly because of their instability in air (see below). The structures of the NHC–boranes **1–3** were unequivocally identified by NMR spectroscopy and mass spectrometry. The <sup>11</sup>B NMR spectra showed sharp and upfield-shifted signals around –10 ppm, thus confirming the formation of tetracoordinated borates by intramolecular coordination of NHC moieties.

To explore the fundamental characteristics of the NHC–borane-substituted thiophene  $\pi$  skeletons, we first investigated the properties and reactivities of **1a** and **1b**. The UV absorption spectra in CH<sub>2</sub>Cl<sub>2</sub> showed that both compounds have weak-shoulder absorption bands at 327 and 312 nm, respectively (Table 1). These derivatives show purple fluo-

**Table 1:** Photophysical Properties of **1–3**.

Compd	Solvent	Absorption <sup>[a]</sup> $\lambda_{\text{abs}}$ [nm]	$\log \epsilon$	Fluorescence $\lambda_{\text{em}}$ [nm]	Stokes shift $\Delta \nu$ [cm <sup>–1</sup> ]
<b>1a</b>	C <sub>6</sub> H <sub>12</sub>	349	2.88	429	5340
	C <sub>6</sub> H <sub>6</sub>	342	3.03	440	6510
	CH <sub>2</sub> Cl <sub>2</sub>	327	3.15	441	7910
	DMSO	327	3.18	443	8000
<b>1b</b>	CH <sub>2</sub> Cl <sub>2</sub>	312	3.94	440	8820
<b>2</b>	CH <sub>2</sub> Cl <sub>2</sub>	425	4.08	477	2570
<b>3</b>	CH <sub>2</sub> Cl <sub>2</sub>	408	3.79	448	2190

[a] The maximum wavelength of the longest absorption band and its molar absorption coefficient were determined by a PeakFit program.

rescences with maxima ( $\lambda_{\text{em}}$ ) at 441 nm for **1a** and 440 nm for **1b**. Thus, the large Stokes shifts of 7900–8800 cm<sup>–1</sup> are one of the features of this skeleton, and are indicative of their significant structural change in the excited state. According to the molecular orbital calculations at the B3LYP/6-31G\* level,<sup>[13]</sup> the HOMO and LUMO of **1a** are mainly localized on the dimesitylthienylborane moiety and the NHC moiety, respectively (see the Supporting Information). The TD-DFT calculation at the same level of theory suggested that the longest absorption band is assignable to the intramolecular charge transfer (ICT) transition from HOMO to LUMO. However, despite the ICT character, no red-shift was observed in the fluorescence when the solvents were changed from nonpolar to polar. Instead, a blue shift was observed in the absorption spectra of **1a** from 349 nm in cyclohexane to 327 nm in DMSO. This negative solvatochromism demonstrates the larger dipole moment of **1a** in the ground state

compared to that in the excited state. The natural population analysis (MP2/6-31G\*\*/B3LYP/6-31G\*)<sup>[14]</sup> demonstrated the zwitterionic character of **1a** in the ground state with the positive charges on the carbene carbon atom (+0.319) and the boron atom (+0.327) and the negative charges on the carbon atom (C2) at the 2 position of thiophene (–0.419) and the *ipso* carbon atoms (C<sub>ipso</sub>) of the mesityl groups (–0.232 and –0.242), respectively. Consequently, **1a** has a large dipole moment of 6.60 Debye.

Notably, **1a** shows a high reactivity under photoirradiation. Thus, upon irradiation of a solution of **1a** in CH<sub>2</sub>Cl<sub>2</sub> with UV light under a nitrogen atmosphere, a photoreaction smoothly took place with a drastic color change from colorless to deep yellow (Figure 2). In the absorption spectra, an intense new band appeared at 429 nm. The monitoring of the reaction by <sup>1</sup>H NMR spectroscopy demonstrated the clean formation of a single product. Based on various kinds of NMR measurements, including not only <sup>1</sup>H and <sup>11</sup>B NMR spectra, but also COSY, HSQC, HMBC, and 2D NOESY (see the Supporting Information), we determined that the product is a thienyl-migrated 7-borabicyclo[4.1.0]hepta-2,4-diene **1a'** (Figure 2a). According to the TD-DFT calculation (B3LYP/6-31G\*), the intense and long-wavelength absorption band of **1a'** can be assigned to the ICT transition from the HOMO that is localized on the borabicyclo[4.1.0]heptadiene skeleton to the LUMO that is localized on the NHC moiety.

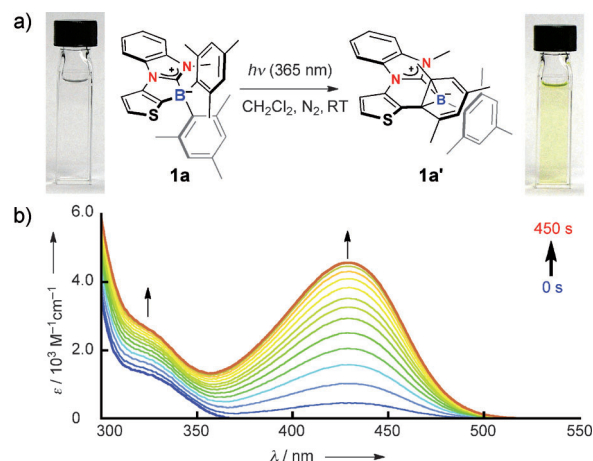


**Figure 2.** a) Photoreaction of **1a** with pictures of the solution before and after irradiation by UV light (365 nm), and b) absorption spectral change of a solution of **1a** in CH<sub>2</sub>Cl<sub>2</sub> (0.03 mM) upon light irradiation.

Recently, Braunschweig and co-workers reported the formation of NHC-coordinated borabicyclo[4.1.0]hepta-2,4-diene derivatives by reduction of BHCl<sub>2</sub>·*IMe* (*IMe* = 1,3-dimethylimidazol-2-ylidene) with sodium naphthalenide in THF.<sup>[15]</sup> In this reaction, the borabicyclo[4.1.0]heptadiene skeleton is likely produced by the [2+1] cycloaddition of an in situ generated borylene with naphthalene. On the other hand, Wang and co-workers have recently pioneered the photoisomerization of 2-(2-borylaryl)-substituted N-heteroaryl compounds, which also affords the borabicyclo[4.1.0]hepta-2,4-diene skeleton.<sup>[16]</sup> Its structure has been unambiguously determined by X-ray crystallography.<sup>[16c]</sup> The photoreaction we now observed can be regarded as

a carbene-analogous reaction of the photoisomerization described by Wang.<sup>[17]</sup> Different from the photoisomerization of the N-heteroaryl-coordinated substrate, the NHC-coordinated product **1a'** emits fluorescence. The fluorescence maximum was shifted from 441 nm for **1a** to 459 nm for **1a'** in CH<sub>2</sub>Cl<sub>2</sub>. In addition, unlike the reaction of the N-heteroaryl-coordinated substrate, the NHC-coordinated product **1a'** does not revert to starting material **1a** under thermal conditions. We confirmed that a chlorobenzene solution of **1a'** remained intact, even after heating at 120 °C for two hours. The high thermal stability of **1a'** results from the more persistent coordination of the NHC to the borabicyclo[4.1.0]heptadiene skeleton.

To gain insights into the mechanism of this reaction, we conducted the structural optimization in the excited state at the B3LYP/def2-SV(P) level (see the Supporting Information). In the local-minimum structure **1a\*** in the S<sub>1</sub> excited state, one of the mesityl groups is located closer to the 2 position of the thiophene moiety compared to the initial ground-state structure (Figure 3). The distance between the C2 atom of the thiophene and the C<sub>ipso</sub> atom of the mesityl group becomes shorter, from 2.588 Å in **1a** to 2.408 Å in **1a\***, accompanied by a narrowing of the C2–B–C<sub>ipso</sub> angle from 101.98° in **1a** to 92.79° in **1a\***. This structural change results from the ICT transition from the HOMO that is largely localized on the mesityl moiety to the LUMO that is localized on the NHC ring, thus reducing the electron density of the C<sub>ipso</sub> atom. From this excited-state structure, the electron-rich thienyl C2 atom should migrate to the electron-poor C<sub>ipso</sub> atom of the mesityl group, followed by the formation of the borabicyclo[4.1.0]heptadiene skeleton, while maintaining the NHC coordination to the boron atom. Thus, an important requisite for this photoreaction is that the HOMO is localized on the electron-rich mesityl moiety in the ground state. Moreover, it is interesting to note that the dibenzoborole derivative **1b** did not undergo the photoisomerization. This result suggests that the rigidity of the dibenzoborole moiety can suppress photoisomerization.

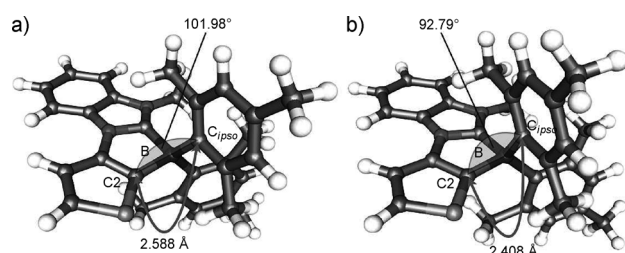


**Figure 3.** Optimized structures of **1a** a) in the ground state, and b) in the S<sub>1</sub> excited state, calculated at the B3LYP/def2-SV(P) level.

We have previously reported that (3-boryl-2-thienyl)-2-thiazole-based  $\pi$ -conjugated system **11** has a characteristic electron-accepting feature, in which the intramolecular coordination of the thiazole to the boron moiety effectively decreases the LUMO level.<sup>[18]</sup> In sharp contrast, notably, we now found that the intramolecular coordination of the NHC to the boron moiety has a totally opposite electronic effect (Figure 4). The calculations showed that the NHC–borane-substituted bithiophene **2'**, which is a model for **2**, has a much higher-lying HOMO (by 0.32 eV) compared with that of a non-borylated congener **12**, while the LUMO level is not significantly influenced by intramolecular coordination. Thus, the NHC–borane moiety is a powerful skeleton to make the  $\pi$  skeleton electron-donating in nature.

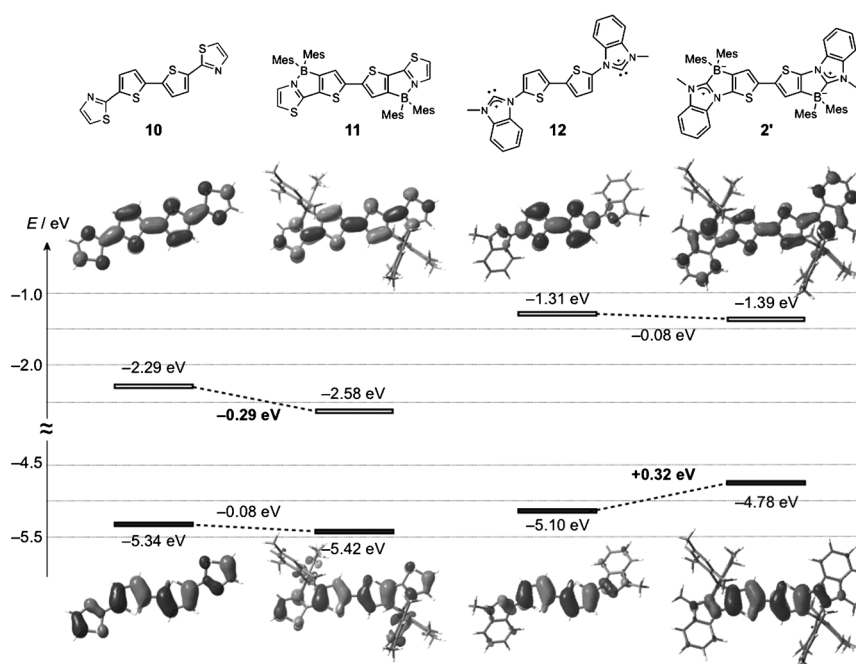


**Figure 4.** Electronic effects of the introduction of boron moieties to a thienylthiazole skeleton and a NHC–borane-substituted thiophene skeleton, calculated at the B3LYP/6-31G\* level.

Bithiophene derivatives **2** and **3** showed interesting electrochemical properties, which reflected the electronic impact of the NHC–borane moiety. Cyclic voltammograms were measured in CH<sub>2</sub>Cl<sub>2</sub> with Bu<sub>4</sub>NPF<sub>6</sub> as a supporting electrolyte (Figure 5). While **3** showed an irreversible oxidation wave with the peak potential  $E_{pc}$  of +0.27 V (vs. Fc/Fc<sup>+</sup>), **2** exhibited a reversible oxidation wave with the half potential  $E_{1/2}$  of +0.28 V. Their low oxidation potentials are consistent with their high HOMO levels (**2**: −4.78 eV; **3**: −4.74 eV), which were obtained by DFT calculations. These compounds are prone to oxidation in air as a result of these low oxidation potentials. The reversible oxidation wave for **2** demonstrates the importance of the substitution pattern for the stabilization of the produced radical cation.

In the absorption spectra in CH<sub>2</sub>Cl<sub>2</sub>, the longest-wavelength absorption bands of **2** and **3** are red-shifted and stronger compared with those of the monothiophene derivatives **1**. The longest  $\lambda_{max}$  values determined by a PeakFit

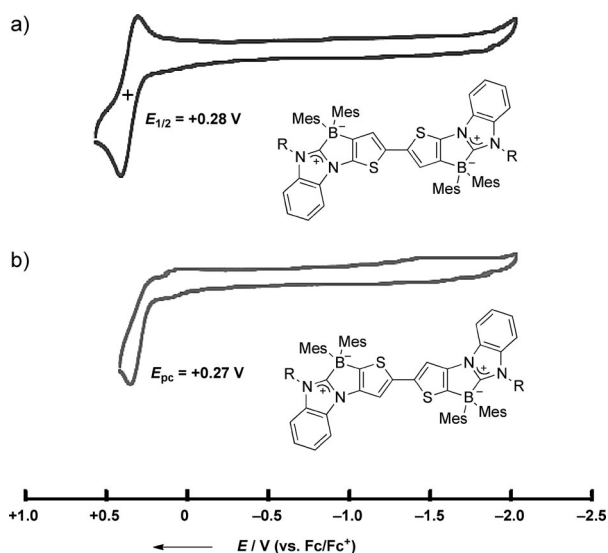


**Figure 5.** Cyclic voltammograms of a) **2** and b) **3** in  $\text{CH}_2\text{Cl}_2$  with  $\text{Bu}_4\text{NPF}_6$  at the scan rate of  $100 \text{ mV s}^{-1}$ .

program are 425 nm and 408 nm, respectively. The fluorescence spectra show that **2** and **3** emit weak sky-blue ( $\lambda_{\text{em}}$  477 nm,  $\Phi_{\text{F}}$  0.05) and blue ( $\lambda_{\text{em}}$  448 nm,  $\Phi_{\text{F}}$  0.02) fluorescences. The crucial difference from the monothiophene derivative **1** is that the bithiophene derivatives are inert to photoisomerization. This behavior is due to the delocalization of their HOMOs, not on the mesityl moieties, but over the bithiophene skeleton. As a result, photoisomerization observed for **1a** no longer proceeds for **2** and **3** (see above). According to the calculations, there is also a notable difference between **2** and **3**. Namely, while the LUMO of **2** is delocalized over the entire NHC–bithiophene framework, that of **3** is mostly localized on the NHC ring (for the pictorial presentation of the LUMO of **3**, see the Supporting Information). The NHC ring serves as the electron-accepting  $\pi$  skeleton, although the LUMO level itself is not particularly low.

We finally succeeded in the crystal structure analysis of the  $\pi$ -expanded bithiophene derivative **2** (Figure 6).<sup>[19]</sup> The boron atoms have a slightly distorted tetrahedral geometry with the sum of the C–B–C bond angles of  $337.7^\circ$ . The length of the NHC C–B coordination bond ( $1.657(3) \text{ \AA}$ ) is compa-

table to those of the known NHC–borane derivatives ( $\approx 1.65 \text{ \AA}$ ).<sup>[20]</sup> The intramolecular coordination of the carbene to the boron atom fixes the thiophene–NHC moiety in a planar fashion. The dihedral angle between the thiophene and NHC rings is  $10.30^\circ$ . In addition, the bithiophene moiety also has a completely planar conformation with the *s-trans* geometry (dihedral angle:  $0.00^\circ$ ). As a consequence of this high planarity, **2** forms a slipped face-to-face  $\pi$ -stacking array. Importantly, in this array, the electron-rich thiophene rings are overlapped with the electron-deficient benzimidazolidene moieties of the adjacent molecules. The interfacial distance of these two rings is about  $3.51 \text{ \AA}$ . Because this overlapping is also observed in the structure of the monothiophene derivative **1a** (see the Supporting Information), the electrostatic interaction between the thiophene and benzimidazolidene moieties may be one of the dominant factors that determine the packing structure.

In summary, we disclosed the multifaceted electronic impacts of the NHC–borane moiety attached to the terminal positions of the thiophene  $\pi$  skeletons. In the monothiophene derivative, photoisomerization smoothly proceeds to give a borabicyclo[4.1.0]-hepta-2,4-diene skeleton. In contrast, the bithiophene derivatives do not undergo the photoreaction and demonstrate interesting electronic properties. The most notable impact of the NHC–borane moiety is its polar and electron-donating character, so that this moiety should be a powerful tool to produce a highly electron-donating  $\pi$ -conjugated skeleton. At the same time, the benzimidazolidene moiety in the terminal NHC–borane unit serves as an electron-deficient moiety, which is beneficial to forming a face-to-face  $\pi$ -stacking array in the solid state through the electrostatic interaction. Making the best use of these characteristics of the NHC–borane moiety would lead to the production of a more fascinating optoelectronic material. Further studies along this line are in progress in our laboratory.

Received: May 24, 2012

Published online: June 22, 2012

**Keywords:** boron · intramolecular coordination · Lewis pairs · N-heterocyclic carbenes ·  $\pi$ -conjugated systems

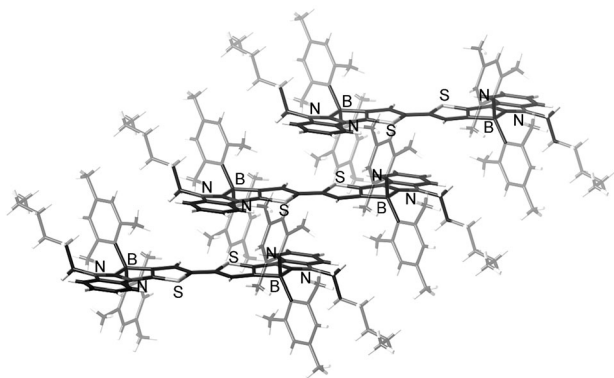


**Figure 6.** Packing structure of **2**.

- [1] a) A. J. Arduengo III, *Acc. Chem. Res.* **1999**, 32, 913; b) D. Bourissou, O. Guerret, F. P. Gabbaï, G. Bertrand, *Chem. Rev.* **2000**, 100, 39; c) F. E. Hahn, M. C. Jahnke, *Angew. Chem.* **2008**, 120, 3166; *Angew. Chem. Int. Ed.* **2008**, 47, 3122; d) T. Dröge, F. Glorius, *Angew. Chem.* **2010**, 122, 7094; *Angew. Chem. Int. Ed.* **2010**, 49, 6940; for donor and acceptor modes of action in NHC organocatalysis, see Scheme 2 in e) X. Bugaut, F. Glorius, *Chem. Soc. Rev.* **2012**, 41, 3511.
- [2] D. P. Curran, A. Solov'yev, M. M. Brahmi, L. Fensterbank, M. Malacria, E. Lacôte, *Angew. Chem.* **2011**, 123, 10476; *Angew. Chem. Int. Ed.* **2011**, 50, 10294.
- [3] a) S.-H. Ueng, M. M. Brahmi, É. Derat, L. Fensterbank, E. Lacôte, M. Malacria, D. P. Curran, *J. Am. Chem. Soc.* **2008**, 130, 10082; b) S.-H. Ueng, L. Fensterbank, E. Lacôte, M. Malacria, D. P. Curran, *Org. Lett.* **2010**, 12, 3002; c) S.-H. Ueng, L. Fensterbank, E. Lacôte, M. Malacria, D. P. Curran, *Org. Biomol. Chem.* **2011**, 9, 3415.



- [4] Q. Chu, M. M. Brahmi, A. Solovyev, S.-H. Ueng, D. P. Curran, M. Malacria, L. Fensterbank, E. Lacôte, *Chem. Eur. J.* **2009**, *15*, 12937.
- [5] J. Monot, M. M. Brahmi, S.-H. Ueng, C. Robert, M. D.-E. Murr, D. P. Curran, M. Malacria, L. Fensterbank, E. Lacôte, *Org. Lett.* **2009**, *11*, 4914.
- [6] a) K.-S. Lee, A. R. Zhugralin, A. H. Hoveyda, *J. Am. Chem. Soc.* **2009**, *131*, 7253; b) H. Wu, S. Radomkit, J. M. O'Brien, A. H. Hoveyda, *J. Am. Chem. Soc.* **2012**, *134*, 8277.
- [7] a) P. A. Chase, D. W. Stephan, *Angew. Chem.* **2008**, *120*, 7543; *Angew. Chem. Int. Ed.* **2008**, *47*, 7433; b) P. A. Chase, A. L. Gille, T. M. Gilbert, D. W. Stephan, *Dalton Trans.* **2009**, 7179; c) D. Holschumacher, T. Bannenberg, C. G. Hrib, P. G. Jones, M. Tamm, *Angew. Chem.* **2008**, *120*, 7538; *Angew. Chem. Int. Ed.* **2008**, *47*, 7428; d) D. Holschumacher, C. Taouss, T. Bannenberg, C. G. Hrib, C. G. Daniliuc, P. G. Jones, M. Tamm, *Dalton Trans.* **2009**, 6927; e) D. Holschumacher, T. Bannenberg, K. Ibrom, C. G. Daniliuc, P. G. Jones, M. Tamm, *Dalton Trans.* **2010**, 39, 10590.
- [8] a) T. Matsumoto, F. P. Gabbaï, *Organometallics* **2009**, *28*, 4252; b) Y. Wang, G. H. Robinson, *Inorg. Chem.* **2011**, *50*, 12326; c) A. Solovyev, S. J. Geib, E. Lacôte, D. P. Curran, *Organometallics* **2012**, *31*, 54.
- [9] a) S.-H. Ueng, A. Solovyev, X. Yuan, S. Geib, L. Fensterbank, E. Lacôte, M. Malacria, M. Newcomb, J. C. Walton, *J. Am. Chem. Soc.* **2009**, *131*, 11256; b) J. C. Walton, M. M. Brahmi, L. Fensterbank, E. Lacôte, M. Malacria, Q. Chu, S.-H. Ueng, A. Solovyev, D. P. Curran, *J. Am. Chem. Soc.* **2010**, *132*, 2350; c) J. Lalevée, S. Telitel, M. A. Tehfe, J. P. Fouassier, D. P. Curran, E. Lacôte, *Angew. Chem.* **2012**, *124*, 6060; *Angew. Chem. Int. Ed.* **2012**, *51*, 5958.
- [10] a) H. Braunschweig, C.-W. Chiu, K. Radacki, T. Kupfer, *Angew. Chem.* **2010**, *122*, 2085; *Angew. Chem. Int. Ed.* **2010**, *49*, 2041; b) K. Nozaki, *Nature* **2010**, *464*, 1136; c) M. Yamashita, *Angew. Chem.* **2010**, *122*, 2524; *Angew. Chem. Int. Ed.* **2010**, *49*, 2474; d) H. Braunschweig, C.-W. Chiu, T. Kupfer, K. Radacki, *Inorg. Chem.* **2011**, *50*, 4247.
- [11] a) T. K. Wood, W. E. Piers, B. A. Keay, M. Parvez, *Angew. Chem.* **2009**, *121*, 4069; *Angew. Chem. Int. Ed.* **2009**, *48*, 4009; b) T. K. Wood, W. E. Piers, B. A. Keay, M. Parvez, *Chem. Eur. J.* **2010**, *16*, 12199.
- [12] X. Zheng, G. E. Herberich, *Organometallics* **2000**, *19*, 3751.
- [13] The DFT calculations were performed by Gaussian 09 program (see the Supporting Information).
- [14] NBO Version 3.1, E. D. Glendening, A. E. Reed, J. E. Carpenter, and F. Weinhold.
- [15] P. Bissinger, H. Braunschweig, K. Kraft, T. Kupfer, *Angew. Chem.* **2011**, *123*, 4801; *Angew. Chem. Int. Ed.* **2011**, *50*, 4704.
- [16] a) Y.-L. Rao, H. Amarne, S.-B. Zhao, T. M. McCormick, S. Martić, Y. Sun, R.-Y. Wang, S. Wang, *J. Am. Chem. Soc.* **2008**, *130*, 12898; b) C. Baik, Z. M. Hudson, H. Amarne, S. Wang, *J. Am. Chem. Soc.* **2009**, *131*, 14549; c) H. Amarne, C. Baik, S. K. Murphy, S. Wang, *Chem. Eur. J.* **2010**, *16*, 4750; d) C. Baik, S. K. Murphy, S. Wang, *Angew. Chem.* **2010**, *122*, 8400; *Angew. Chem. Int. Ed.* **2010**, *49*, 8224; e) H. Amarne, C. Baik, R.-Y. Wang, S. Wang, *Organometallics* **2011**, *30*, 665; f) Y.-L. Rao, S. Wang, *Inorg. Chem.* **2011**, *50*, 12263.
- [17] Wang and co-workers have also recently found a similar photoisomerization of NHC–boranes: Y.-L. Rao, L. D. Chen, N. J. Mosey, S. Wang, *J. Am. Chem. Soc.*, in press.
- [18] A. Wakamiya, T. Taniguchi, S. Yamaguchi, *Angew. Chem.* **2006**, *118*, 3242; *Angew. Chem. Int. Ed.* **2006**, *45*, 3170.
- [19] CCDC 883071 (**1a**) and 883072 (**2**) contain the supplementary crystallographic data for this paper. These data can be obtained free of charge from The Cambridge Crystallographic Data Centre via [www.ccdc.cam.ac.uk/data\\_request/cif](http://www.ccdc.cam.ac.uk/data_request/cif).
- [20] a) C. Lambert, I. Lopez-Solera, P. R. Raithby, *Organometallics* **1996**, *15*, 452; b) M. Tamm, T. Lügger, F. E. Hahn, *Organometallics* **1996**, *15*, 1251; c) A. C. Filippou, O. Chernov, K. W. Stumpf, G. Schnakenburg, *Angew. Chem.* **2010**, *122*, 3368; *Angew. Chem. Int. Ed.* **2010**, *49*, 3296.